An Integrated Flexible Platform of Electromagnetic Metamaterials and Acoustofluidics on Kapton

Shahrzad Zahertar[1], Jiaen Wu[2,3], Xiang-Zhong Chen[2], Salvador Pane[2], Olgac Ergeneman[3], Yong-Qing Fu[1], Hamdi Torun[1]

[1]Department of Mathematics, Physics and Electrical Engineering, Northumbria University, Newcastle upon Tyne, UK
[2]Institute of Robotics and Intelligent Systems, ETH Zürich, Zurich, Switzerland
[3] Magnes AG, Zurich, Switzerland
s.zahertar@northumbria.ac.uk

2021 IEEE International Conference on Flexible and Printable Sensors and Systems (FLEPS) | 978-1-7281-9173-7/20/$31.00 ©2021 IEEE | DOI: 10.1109/FLEPS51544.2021.9469821

***Abstract*— Electromagnetic metamaterial-based sensors are promising for wide-range of applications due to their high quality factors and their simple structure designs. On the other hand, surface acoustic wave (SAW)-based actuators have been studied for their capabilities in manipulating microfluids. In this paper, we propose a single flexible structure that can act as a metamaterial-based sensor in microwave frequencies, as well as a SAW actuator in radio frequencies. This feature makes our proposed design suitable for an integrated platform for both sensing and acoustofluidic manipulation purposes.**

Keywords—Metamaterials; split-ring resonators; surface acoustic waves, sensors and actuators;

I. Introduction

Metamaterials are artificially engineered structures that possess unique properties which are not readily available in nature, e.g. achieving a negative refractive index and the capability of manipulating electromagnetic waves [1], [2]. Split-ring resonators (SRRs) that are basically sub-wavelength metallic rings with one or more splits are among the basic building blocks of metamaterials [3]. Circular and rectangular SRRs fabricated on a dielectric substrate are resonant devices with high quality factors that have been extensively studied for sensing applications [4]–[9] attributed to their simple design, ease of fabrication, and high sensitivity. Another advantage of SRRs is that they can be excited wirelessly under various electromagnetic configurations [6], [10]. The fundamental magnetic resonant frequency of the SRRs depends mainly on their geometry and dielectric properties of their surroundings and can be modelled using lumped components [11] ($f=1/\sqrt{(L_{eff}C_{eff})}$, where f is the fundamental magnetic resonance, L_{eff} is the effective conductance, and C_{eff} is the effective capacitance of the structure). Altering any of these components by changing the geometry of the resonator or the dielectric properties of the medium results in a change in the resonant frequency of the structure, and this phenomenon can be utilized as a sensing mechanism.

On the other hand, surface acoustic wave (SAW) actuators are composed of interdigital transducers (IDTs), which are fabricated on a piezoelectric layer and have been investigated for their microfluidic actuation capabilities to achieve multiple functions such as streaming [12]–[14], pumping [15], [16], jetting and nebulization [17].

The concept proposed in this paper is based on our previous studies [18]–[20], and our objective in this paper is to implement our idea of combining metamaterial-based resonators and SAW-based actuators on a flexible substrate using a single structure. To this end, we have designed a similar structure that we reported in [20] and fabricated it on a thin film of Kapton, a commercially available form of polyimide (PI) film [21]. We explored its capability to be used as an SRR-based sensor in microwave frequencies, and also to be used as a SAW actuator in radio frequencies (RF), when it is pressed on piezoelectric substrate.

II. Methodology

Our device is composed of 40 pairs of IDTs made of Ti/Au with the thicknesses of 10/100 nm and are developed on a 120µm-thick film of Kapton through the standard photolithography and lift-off processes. A schematic of the fabricated device is shown in Fig.1.

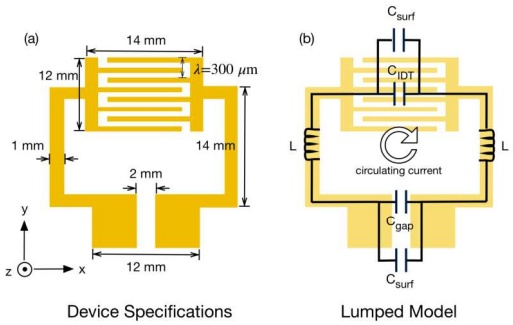

Fig. 1. A schematic of the (a) fabricated device and its specifications (b) lumped model of the device as an SRR-based structure.

We used CST Studio Suite, a commercially available electromagnetic simulation software, for the design of the structures. Planar waveguides were utilized to excite the device under various directions of electric and magnetic fields between 3.5-5 GHz range. Scattering parameters and current density patterns were obtained for a specific excitation condition.

For electromagnetic characterization, a copper loop antenna with a perimeter of 8.8 cm was connected to one port of a vector network analyzer (Agilent Technologies, N5230A) and was utilized to interrogate the fabricated structure. Reflection coefficient (S_{11}) of the device was monitored in S-band. For sensing experiments, four concentrations of sodium chloride (NaCl) ranging from 1 M

up to 4 M were prepared. A droplet of 40 µL of each concentration was placed on the gap between the electrode pads of the structure. These experiments were performed sequentially and were repeated at least for five times, and S_{11} was measured each time after loading the droplet on the device.

For acoustic characterization of the device in radio frequencies, the fabricated device was pressed onto a 128° Y-cut lithium niobate substrate from the electrode side and the electrode pads of the structure were connected to one port of a vector network analyzer (Keysight N9913A) and S_{11} was recorded. For actuation experiments, a signal generator (Aim TTi, TG5011A) was used to apply power through an amplifier (Amplifier Research, model 75A250) to the electrodes of the structure. A droplet of 2 µL of deionized water (DI) containing polystyrene microbeads (with diameter of 10 µm) was placed in front of the IDTs and an RF power of 7 W at 10.24 MHz was applied to the electrodes. Streaming was recorded using a conventional CMOS camera. Motion of the particles inside the droplet and streamlines were captured using PIVLab tool in MATLAB, which is a digital particle velocimetry method [22].

III. Electromagnetic Characteristics

A. Electromagnetic Chracterisation

We experimentally characterized the fabricated device in a band of 3.5-5 GHz and compared the results to the simulations as shown in Fig. 2. In the simulated model, we set the boundary condition so that electromagnetic wave propagation is along x-axis, electric field is along y-axis, and magnetic field is perpendicular to the device. This excitation condition excites a magnetic resonance at 4.4 GHz and results in two circulating current paths on the right and left sides of the device. The current density pattern and excitation configuration are shown in the inset of Fig. 2. In the experimental setting, we obtained a resonance at 4.3 GHz.

As can be seen from the Fig. 2, the simulation and the experiment results are in good agreement with each other. The slight discrepancy between the simulation and the experiment data could be due to the differences in the nominal values loaded from the library in the simulations and the actual properties of the fabricated device and the environment in the experimental setting.

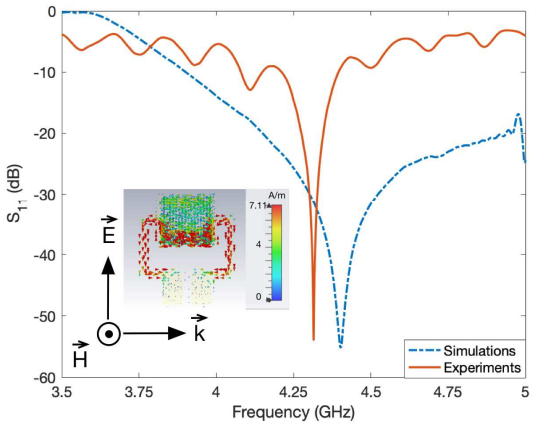

Fig. 2. Reflection coefficient (S_{11}) spectra of the simulation and the experimental data. The inset illustrates the current density patterned obtained from the simulations at 4.4 GHz.

B. Electromagnetic Sensing

For sensing experiments, we prepared four different solutions of NaCl including 1, 2, 3, 4 molars. We placed a 40 µL droplet of deionized water and also the prepared NaCl solutions with four different concentrations, in sequence, on the gap of the electrode pads and recorded the S_{11} spectra. To ensure the reliability of the data, we repeated the experiments for at least five times for each concentration. The obtained results are shown in Fig. 3.

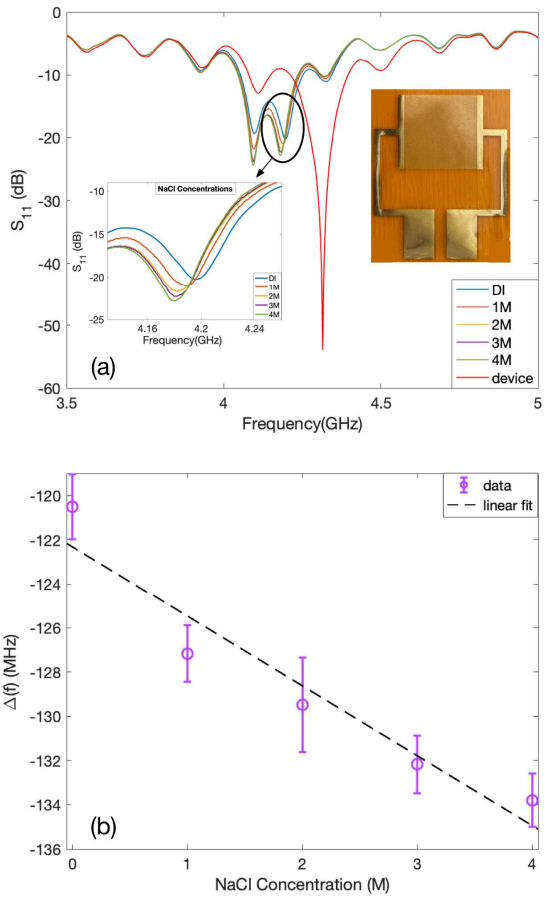

Fig. 3. (a) S_{11} spectra of various NaCl concentrations, DI, and the device for a sample set of experiments (b) the shifts in the resonance of the device after loading a droplet of each concentration on the device.

Loading a droplet on the gap area of the structure alters the circulating current around the geometry of the resonator (shown in inset to Fig. 2). The experimental study revealed a shift in the resonant frequency of the device towards lower values. The conductivity and the dielectric permittivity of the resonator area where the droplet is placed are altered, leading to a decrease in resonant frequency with increasing concentration. Fig. 3(a) shows a set of sensing experiments and the S_{11} spectra that were obtained for various concentrations (The fabricated device is also shown in the inset of this graph). Fig.3 (b) represents the shifts in the frequency that were achieved by loading a droplet of each concentration and the error bars indicate the standard deviation from the average shift. The calculated sensitivity of the device is ~3 MHz/M.

IV. ACOUSTOFLUIDIC CHARACTERISTICS

To characterize the acoustofluidics performance of our device, we followed our method explained in ref [20] where we physically attached the fabricated device on a lithium niobate substrate ($LiNbO_3$) from the electrode side by applying contact force. We then connected the electrode pads to one port of the network analyzer and recorded the reflection coefficient. The acoustic frequency of the device depends on the phase velocity of acoustic waves in the substrate and the wavelength of the IDTs ($f=v/\lambda$, f as the fundamental resonance, v as the phase velocity of acoustic waves in the substrate, and λ is the wavelength of IDTs).

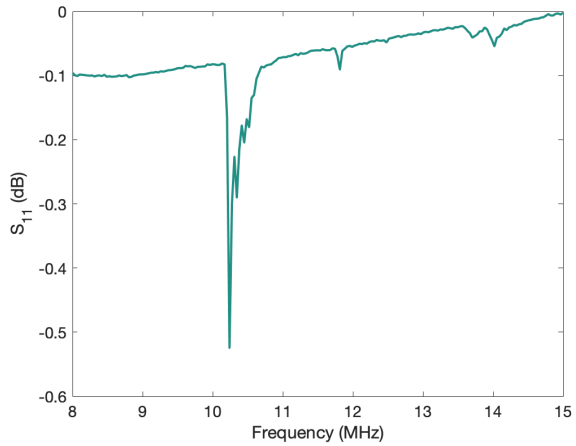

Fig. 4. Acoustic characterization of the fabricated device.

The nominal phase velocity of acoustic waves in a $LiNbO_3$ substrate is ~3980 m/s, and the designed wavelength of the IDTs in the fabricated structure is 300 µm. We measured the S_{11} spectrum as shown in Fig. 4 indicating an acoustic resonance at 10.24 MHz. This resonance matches our design parameters considering that the IDTs of the structure are in contact with the $LiNbO_3$ substrate through physical attachment and the actual phase velocity would be lower than the nominal value. For performing actuation experiments in our experimental setup, we diluted polystrene particles inside DI water and placed a droplet with a 2 µL of this solution in front of the IDTs. We then applied a power of 7 W to electrode pads at 10.24 MHz via a signal generator and a power amplifier.

The recorded motion of the particles and the obtained streamlines that were analyzed by PIVLab are shown in Fig. 5 (a-d) from the beginning towards the end of the experiment.

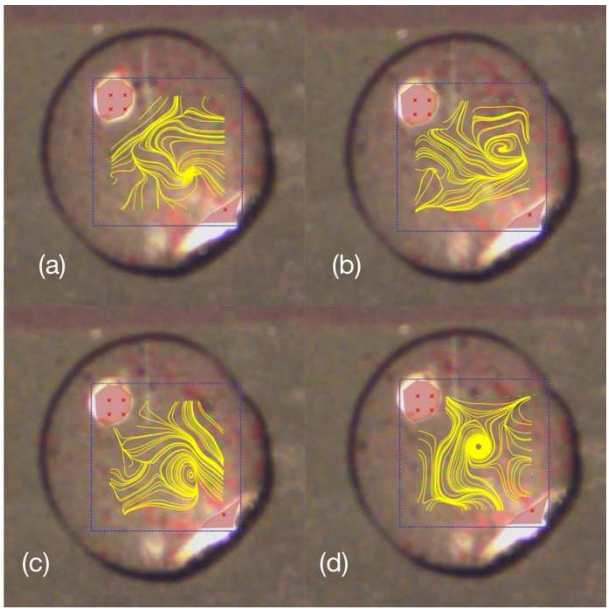

Fig. 5. Streaming patterns of the polystyrene particles inside of a 2 µL droplet at applied power of 7 W at 10.24 MHz, captured at (a) 5.5 s, (b) 17.6 s, (c) 24.8 s, (d) 27.5 s in a 29 s experiment, respectively.

Fig. 5 shows the streamlines captured at randomly selected time instances at 5.5, 17.6, 24.8, 27.5 s in an experiment lasted 29 s.

V. CONCLUSIONS

In this paper, we proposed the idea of combining metamaterial-based resonators with SAW-based actuators using a single structure on a flexible Kapton film. We characterized our device electromagnetically and used it as an SRR to perform sensing experiments. We also characterized our device acoustically by pressing this flexible structure onto a lithium niobate substrate and achieved streaming at its acoustic resonance. The fabricated device has the potential to be integrated into lab-on-chip devices for its dual-functionality in both sensing an actuation on a single geometry. The sensing and actuation functionalities are based on two different mechanisms and are realized at different frequencies. Decoupling the operation frequencies are also advantageous as readout electronics and the driving electronics can be optimized separately without cross-talk problems. Also, these flexible substrates are promising to be integrated into flexible electronics and wearable devices in the future.

ACKNOWLEDGMENT

This project has received funding from the ATTRACT project funded by the EC under Grant Agreement 777222 and the Engineering Physics and Science Research Council of UK (EPSRC EP/P018998/1).

REFERENCES

[1] V. G. Veselago, 'Electrodynamics of substances with simultaneously negative and', *Usp. Fiz. Nauk*, vol. 92, p. 517, 1967.

[2] J. B. Pendry, A. J. Holden, D. J. Robbins, and W. J. Stewart, 'Magnetism from conductors and enhanced nonlinear phenomena', *IEEE transactions on microwave theory and techniques*, vol. 47, no. 11, pp. 2075–2084, 1999.

[3] D. R. Smith, W. J. Padilla, D. C. Vier, S. C. Nemat-Nasser, and S. Schultz, 'Composite medium with simultaneously negative permeability and permittivity', *Physical review letters*, vol. 84, no. 18, p. 4184, 2000.

[4] G. Ekinci, A. D. Yalcinkaya, G. Dundar, and H. Torun, 'Split-ring resonator-based strain sensor on flexible substrates for glaucoma detection', in *Journal of Physics: Conference Series*, 2016, vol. 757, no. 1, p. 012019.

[5] S. Zahertar, L. E. Dodd, and H. Torun, 'Embroidered rectangular split-ring resonators for material characterisation', in *2019 IEEE International Conference on Flexible and Printable Sensors and Systems (FLEPS)*, 2019, pp. 1–3.

[6] H. Torun, F. Cagri Top, G. Dundar, and A. D. Yalcinkaya, 'An antenna-coupled split-ring resonator for biosensing', *Journal of Applied Physics*, vol. 116, no. 12, p. 124701, 2014.

[7] W. Withayachumnankul, K. Jaruwongrungsee, A. Tuantranont, C. Fumeaux, and D. Abbott, 'Metamaterial-based microfluidic sensor for dielectric characterization', *Sensors and Actuators A: Physical*, vol. 189, pp. 233–237, 2013.

[8] H.-J. Lee *et al.*, 'A planar split-ring resonator-based microwave biosensor for label-free detection of biomolecules', *Sensors and Actuators B: Chemical*, vol. 169, pp. 26–31, 2012.

[9] S. P. Chakyar, S. K. Simon, C. Bindu, J. Andrews, and V. P. Joseph, 'Complex permittivity measurement using metamaterial split ring resonators', *Journal of Applied Physics*, vol. 121, no. 5, p. 054101, 2017.

[10] S. Zahertar, A. D. Yalcinkaya, and H. Torun, 'Rectangular split-ring resonators with single-split and two-splits under different excitations at microwave frequencies', *AIP Advances*, vol. 5, no. 11, p. 117220, Nov. 2015, doi: 10.1063/1.4935910.

[11] O. Sydoruk, E. Tatartschuk, E. Shamonina, and L. Solymar, 'Analytical formulation for the resonant frequency of split rings', *Journal of applied physics*, vol. 105, no. 1, p. 014903, 2009.

[12] A. Wixforth, C. Strobl, C. Gauer, A. Toegl, J. Scriba, and Z. v Guttenberg, 'Acoustic manipulation of small droplets', *Analytical and bioanalytical chemistry*, vol. 379, no. 7–8, pp. 982–991, 2004.

[13] R. Shilton, M. K. Tan, L. Y. Yeo, and J. R. Friend, 'Particle concentration and mixing in microdrops driven by focused surface acoustic waves', *Journal of Applied Physics*, vol. 104, no. 1, p. 014910, 2008.

[14] A. Wixforth, 'Acoustically driven programmable microfluidics for biological and chemical applications', *JALA: Journal of the Association for Laboratory Automation*, vol. 11, no. 6, pp. 399–405, 2006.

[15] Z. Guttenberg *et al.*, 'Planar chip device for PCR and hybridization with surface acoustic wave pump', *Lab on a Chip*, vol. 5, no. 3, pp. 308–317, 2005.

[16] M. Baudoin, P. Brunet, O. Bou Matar, and E. Herth, 'Low power sessile droplets actuation via modulated surface acoustic waves', *Applied Physics Letters*, vol. 100, no. 15, p. 154102, 2012.

[17] Y. Q. Fu *et al.*, 'Advances in piezoelectric thin films for acoustic biosensors, acoustofluidics and lab-on-chip applications', *Progress in Materials Science*, vol. 89, pp. 31–91, Aug. 2017, doi: 10.1016/j.pmatsci.2017.04.006.

[18] S. Zahertar, Y. Wang, R. Tao, J. Xie, Y. Q. Fu, and H. Torun, 'A fully integrated biosensing platform combining acoustofluidics and electromagnetic metamaterials', *J. Phys. D: Appl. Phys.*, vol. 52, no. 48, p. 485004, Nov. 2019, doi: 10.1088/1361-6463/ab3f7d.

[19] R. Tao *et al.*, 'Flexible and Integrated Sensing Platform of Acoustic Waves and Metamaterials based on Polyimide-Coated Woven Carbon Fibers', *ACS sensors*, vol. 5, no. 8, pp. 2563–2569, 2020.

[20] S. Zahertar *et al.*, 'A Flexible PVDF-based Platform Combining Acoustofluidics and Electromagnetic Metamaterials', in *2020 IEEE International Conference on Flexible and Printable Sensors and Systems (FLEPS)*, 2020, pp. 1–4.

[21] 'DuPont™ Kapton® polyimide films'. https://www.dupont.com/electronic-materials/kapton-polyimide-film.html (accessed Mar. 13, 2021).

[22] W. Thielicke and E. Stamhuis, 'PIVlab–towards user-friendly, affordable and accurate digital particle image velocimetry in MATLAB', *Journal of open research software*, vol. 2, no. 1, 2014.